THE JOURNAL OF BIOLOGICAL CHEMISTRY VOL. 287, NO. 12, pp. 9640–9650, March 16, 2012


# Augmentation of Kv4.2-encoded Currents by Accessory Dipeptidyl Peptidase 6 and 10 Subunits Reflects Selective Cell Surface Kv4.2 Protein Stabilization*[S]

Received for publication, November 15, 2011, and in revised form, January 28, 2012 Published, JBC Papers in Press, February 6, 2012, DOI 10.1074/jbc.M111.324574

**Nicholas C. Foeger**[1], **Aaron J. Norris**[2], **Lisa M. Wren, and Jeanne M. Nerbonne**[3]

*From the Department of Developmental Biology Washington University School of Medicine, St. Louis, Missouri 63110*

**Background:** Somatodendritic Kv4-encoded A-Type $K^+$ current densities are enhanced by both cytosolic $K^+$ channel interacting proteins (KChIPs) and transmembrane dipeptidyl peptidases (DPPs).
**Results:** DPPs selectively stabilize cell surface Kv4 protein expression, whereas KChIPs stabilize total and surface Kv4 protein expression.
**Conclusion:** DPPs regulate Kv4-encoded current densities through mechanisms distinct from the KChIPs.
**Significance:** Multiple mechanisms determine functional Kv4 channel densities.

**Rapidly activating and inactivating somatodendritic voltage-gated $K^+$ (Kv) currents, $I_A$, play critical roles in the regulation of neuronal excitability. Considerable evidence suggests that native neuronal $I_A$ channels function in macromolecular protein complexes comprising pore-forming ($\alpha$) subunits of the Kv4 subfamily together with cytosolic, $K^+$ channel interacting proteins (KChIPs) and transmembrane, dipeptidyl peptidase 6 and 10 (DPP6/10) accessory subunits, as well as other accessory and regulatory proteins. Several recent studies have demonstrated a critical role for the KChIP subunits in the generation of native Kv4.2-encoded channels and that Kv4.2-KChIP complex formation results in mutual (Kv4.2-KChIP) protein stabilization. The results of the experiments here, however, demonstrate that expression of DPP6 in the mouse cortex is unaffected by the targeted deletion of Kv4.2 and/or Kv4.3. Further experiments revealed that heterologously expressed DPP6 and DPP10 localize to the cell surface in the absence of Kv4.2, and that co-expression with Kv4.2 does *not* affect total or cell surface DPP6 or DPP10 protein levels. In the presence of DPP6 or DPP10, however, cell surface Kv4.2 protein expression is selectively increased. Further addition of KChIP3 in the presence of DPP10 markedly increases total and cell surface Kv4.2 protein levels, compared with cells expressing only Kv4.2 and DPP10. Taken together, the results presented here demonstrate that the expression and localization of the DPP accessory subunits are independent of Kv4 $\alpha$ subunits and further that the DPP6/10 and KChIP accessory subunits independently stabilize the surface expression of Kv4.2.**

Rapidly activating and inactivating somatodendritic voltage-gated $K^+$ (Kv)[4] currents, typically referred to as $I_A$ (1, 2), regulate action potential repolarization (3, 4) and repetitive firing (5–8) in cortical and hippocampal pyramidal neurons and prevent backpropagation into dendrites (9–12). Increasing evidence suggests that native neuronal $I_A$ channels function in macromolecular protein complexes comprising Kv4 pore-forming ($\alpha$) subunits, together with Kv4 channel accessory subunits, including the $K^+$ channel interacting proteins (KChIP1–4), dipeptidyl peptidases 6 and 10 (DPP6 and DPP10), and additional regulatory and scaffolding proteins (13–19). Interestingly, recent studies have identified DPP6 and DPP10 as genes associated with autism (20), as well as amyotrophic lateral sclerosis (21, 22), although the pathogenic mechanisms remain to be elucidated.

The KChIPs, initially identified as Kv4 channel accessory subunits in a yeast two-hybrid screen (17), are cytosolic, calcium-binding proteins that are members of the neuronal calcium sensor protein family (23). Co-expression with KChIPs increases the densities and alters the time- and voltage-dependent properties of Kv4 $\alpha$ subunit-encoded currents (17, 24–26). The accessory DPP6 and 10 subunits, in contrast, are transmembrane proteins (27) with high homology to the serine peptidase DPP4 (also referred to as CD26), but they lack proteolytic activity (28). Similar to the KChIPs, co-expression with DPP6 or DPP10 alters the properties and densities of Kv4-encoded currents (15, 29–31). The finding that DPP6 increases the conductance of single Kv4.2-encoded channels has been interpreted as suggesting a potential mechanism for increasing Kv4.2 current densities (32), although co-expression with DPP subunits also results in the redistribution of the Kv4.2 protein to the cell surface (29, 33). Recent studies also suggest a physiological role for DPP6 in maintaining the gradient of $I_A$ expression in the dendrites of hippocampal pyramidal neurons (34).

Several previous studies also suggest a critical role for the KChIPs in the generation of native Kv4-encoded channels and

* This work was supported, in whole or in part, by National Institutes of Health Grant HL034161 (to J. M. N.).
[S] This article contains supplemental Fig. S1.
[1] Supported by Grant T32-HL007275 from the NHLBI, National Institutes of Health.
[2] Supported by Grant T32-EY013360 from the National Eye Institute.
[3] To whom correspondence should be addressed: Dept. of Developmental Biology, Washington University School of Medicine, Campus Box 8103, 660 South Euclid Ave., St. Louis, MO 63110. Tel.: 314-362-2564; Fax: 314-362-7058; E-mail: jnerbonne@wustl.edu.

[4] The abbreviations used are: Kv, voltage-gated $K^+$; KChIP, $K^+$ channel interacting protein; DPP, dipeptidyl peptidase; YFP, yellow fluorescent protein.

that Kv4-KChIP protein-protein interactions are required for the stability of both proteins (25, 35–39). Interestingly, a similar stabilizing effect has been described for the *Shaker* channel accessory subunit, *Sleepless*, in *Drosophila* (40). In contrast, the biochemical experiments detailed here demonstrate that neither total nor cell surface DPP6/10 protein expression is affected by the presence of Kv4.2. Indeed, DPP6 and DPP10 traffic to the cell surface in the absence of Kv4 $\alpha$ subunits. In addition, although not affecting total Kv4.2 protein, DPP6/10 selectively increase cell surface Kv4.2 expression. When KChIP3 is expressed in the presence of DPP10, however, total and cell surface Kv4.2 protein are increased and to the same extent as in the absence of DPP10.

## EXPERIMENTAL PROCEDURES

*Plasmid Construct Generation*—The constructs encoding tdTomato alone (AdloxCRI) or tdTomato with WT Kv4.2 (AdloxCRI.mKv4.2) or Kv4.2Δ40N (AdloxCRI.mKv4.2Δ40N) have been described previously (25). In brief, the AdEGI vector (41) (a gift from D. C. Johns) is a bi-cistronic adenoviral shuttle vector expressing enhanced GFP and a second open reading frame separated by an internal ribosomal entry site in a single transcript driven by the ecdysone promoter. The ecdysone promoter region, together with enhanced GFP, was excised using site-directed mutagenesis followed by restriction endonuclease digestion, as previously described (25), and the coding sequence for the CMV promoter, together with the red fluorescent protein tdTomato (42) (a gift from R. Y. Tsien), was substituted to generate the vector AdloxCRI.

The coding sequence for mouse *Kcnd2* (NM_019697) (Kv4.2) was cloned into AdloxCRI at the SacI and EcoRI restriction sites to generate the vector AdloxCRI.mKv4.2. The Kv4.2 N-terminal truncation construct (Kv4.2Δ40N) was generated in which amino acids 2–40 were deleted by PCR cloning of truncated Kv4.2 sequence from AdloxCRI.mKv4.2 with 5′ SacI and 3′ EcoRI restriction sites using the following primers: 5′-actacgagctcatggctctgatagtgctgaa and 3′-gccgtgaattcttacaaagcagacaccctg. The Kv4.2Δ40N truncation construct was then cloned into AdloxCRI between the SacI and EcoRI restriction sites. In addition, the alanine residue at position 235 of Kv4.2 was mutated to valine (Kv4.2A235V) by site-directed mutagenesis of AdloxCRI.mKv4.2 using a QuikChange XL kit (Stratagene, Santa Clara, CA) with the following primers: 5′-cttctgcttggataccgtctgtgtcatgatcttca and 3′-tgaagatcatgacacagacggtatccaagcagaag. The construct was sequenced prior to use; no unintentional mutations were identified.

The *Dpp6* sequence (BC048383), which encodes mouse DPP6, was obtained from Open Biosystems (Thermo Fisher Scientific, Huntsville, AL) and was cloned into the pEYFP-N1 vector (Clontech, Mountain View, CA) at the SalI and BamHI restriction sites to generate DPP6-EYFP-N1. The *Dpp10* sequence (BC067026), which encodes mouse DPP10, also obtained from Open Biosystems, was cloned also into pEYFP-N1 at the XhoI and SacII restriction sites to generate DPP10-EYFP-N1. In addition, the *Dpp6* and *Dpp10* coding sequences were subsequently cloned into pCMV-Script (Stratagene) at the BamHI and SalI restriction sites to generate untagged constructs, CMV-Script.DPP6 and CMV-Script.DPP10. The *Kcnip3* coding sequence (BC026980, Open Biosystems), which encodes mouse KChIP3, was also cloned into pEYFP-N1 at the EcoRI and SacII restriction sites to generate KChIP3-EYFP-N1. All of the constructs were sequenced prior to use; no unintentional mutations were introduced by PCR.

*Cell Culture and Transient Transfections*—HEK-293 cells, obtained from the American Tissue Culture Collection (Manassas, VA), were maintained and passaged as previously described (25). In brief, HEK-293 cells were maintained in DMEM (Invitrogen) supplemented with 5% horse serum (Invitrogen), 5% heat-inactivated FCS (Invitrogen),and 1 unit/ml penicillin-streptomycin (Invitrogen). The cells were passaged at confluence every 2–3 days by brief trypsinization (43).

For experiments, the plasmids were mixed with Lipofectamine 2000 (Invitrogen) in Opti-MEM (Invitrogen) and incubated at room temperature for ~30 min prior to the addition to the cultures. For electrophysiology, the cells were transfected in 35-mm dishes using 2 $\mu$g of Lipofectamine mixed with 0.5 $\mu$g of total plasmids. For biochemistry, the cells were transfected in 25-cm$^2$ flasks using 4 $\mu$g of Lipofectamine mixed with 4 $\mu$g of total plasmids. For both physiology and biochemistry, the WT (or mutant) Kv4.2 plasmid was mixed with Adlox.CRI or with one of the Kv accessory subunit DPP6-YFP, DPP10-YFP, or KChIP3 plasmids in a 1:1 ratio. Approximately 8 h later, the plasmid-containing medium was removed and replaced with normal cell culture medium (see above). Electrophysiological recordings and biochemical studies were performed 24–36 h after transfections. Images of transiently transfected (unfixed) HEK-293 cells were also obtained within 36 h of transfections on a Nikon Eclipse TE-2000 E microscope (Nikon Instruments, Melville, NY) using a CoolSNAP HQ$^2$ Camera (Photometrics, Tucson, AZ) interfaced to a Dell (Precision T5400) personal computer running Volocity 5.5 (PerkinElmer Life Sciences).

*Surface Immunohistochemical Staining*—For immunohistochemical experiments, 1 $\mu$g of the DPP6-YFP, DPP10-YFP or KChIP3-YFP plasmid (in the absence of tdTomato) was mixed with 3 $\mu$l of PepMute Transfection Reagent (SignaGen Laboratories, Rockville, MD) and 100 $\mu$l of PepMute Buffer and incubated at room temperature for ~15 min prior to addition to the cells, plated on 35-mm dishes. The cultures were split 5 h later in fresh cell culture medium (see above) and plated onto poly-L-lysine-coated glass coverslips in 12-well plates.

Approximately 48 h after transfections, the medium was replaced with one containing 20 $\mu$M HEPES and rabbit polyclonal anti-GFP (Millipore, Billerica, MA) and incubated at room temperature for 1 h; the cells were washed with PBS (136 mmol/liter NaCl, 2.6 mmol/liter KCl, 10 mmol/liter $NaH_2PO_4$, 1.7 mmol/liter $KH_2PO_4$, pH 7.4) and fixed with 4% paraformaldehyde in PBS for 15 min. The cells were then washed with PBS and incubated with goat anti-rabbit Alexa 555-conjugated secondary antibody (Invitrogen) at room temperature for 90 min, washed with PBS, and coverslipped using ProLong Gold mounting reagent (Invitrogen). The cells were imaged as described above, and line scan intensity histograms of YFP and Alexa 555 fluorescence from individual DPP6-YFP-, DPP10-YFP-, and KChIP3-YFP-expressing cells were obtained using Volocity 5.5 (PerkinElmer Life Sciences). The raw intensities

were normalized to the maximal intensity in the same cell, and the mean ± S.E. normalized intensities were determined.

*Electrophysiology*—Whole cell recordings were obtained from transiently transfected HEK-293 cells as previously described (25). In brief, whole cell recordings were obtained at room temperature (22–24 °C) within 36 h of transfections using an Axopatch-1D amplifier (Axon Instruments, Sunnyvale, CA) interfaced to a Dell (Precision T5400) personal computer using a Digidata 1322A A/D converter (Axon Instruments). Voltage clamp paradigms were controlled, and data were collected using Clampex 9.2 (pClamp 9; Axon Instruments). The data were acquired at 100 kHz, and current signals were filtered on-line at 5 kHz prior to digitization and storage. Recording pipettes contained 115 mM KCl, 20 mM KOH, 10 mM EGTA, 10 mM HEPES, and 5 mM glucose, pH 7.2 (300–310 mOsm). Pipette resistances were 1.5–3.0 MΩ when filled with the recording solution. The bath solution contained 140 mM NaCl, 4 mM KCl, 2 mM $MgCl_2$, 1 mM $CaCl_2$, 10 mM HEPES, and 5 mM glucose, pH 7.4 (300–310 mOsm).

After establishing the whole cell configuration, ± 10 mV steps from a holding potential of −70 mV were applied to allow measurements of whole cell membrane capacitances and input resistances. Whole cell membrane capacitances and series resistances were routinely compensated (≥85%) electronically. Only data obtained from cells with input resistances ≥300 MΩ were analyzed. Leak currents were always <200 pA and were not corrected. Voltage-gated Kv4-encoded $K^+$ currents, evoked in response to 450-ms depolarizing voltage steps to potentials between −60 and + 40 mV from an holding potential of −70 mV, were recorded; voltage steps were presented in 10-mV increments at 10-s intervals.

Electrophysiological data were analyzed using Clampfit 9.2 (Axon). Whole cell membrane capacitances were calculated by integrating the capacitive transients elicited during the + 10-mV voltage steps from the holding potential. Kv4-encoded currents at each test potential were measured as the difference between the maximal outward current amplitude and the current remaining at the end of the 450-ms voltage step. All of the electrophysiological and imaging data are presented as the means ± S.E. The statistical significance of observed differences between groups of cells was evaluated using a Student's *t* test; *p* values are presented in the text, and statistical significance was set at the $p < 0.05$ level.

*Western Blot Analysis*—Using previously described methods (44), total protein lysates were prepared from HEK-293 cells transfected with the Kv4 and Kv accessory subunit plasmids as described above. Transfected cells were scraped from 25-$cm^2$ tissue culture flasks and briefly vortexed in 500 μl of ice-cold lysis buffer: PBS containing protease inhibitor mixture tablet (Roche) and Triton X-100 (1%). After a 15-min incubation with slow rotation at 4 °C, the insoluble fraction was removed by centrifugation at 3000 rpm for 10 min at 4 °C.

For the isolation of cortical tissue for biochemical analyses, the mice were anesthetized with isoflorane and decapitated, and the brains rapidly removed. The posterior (~1 mm) cortex was dissected and flash frozen in liquid nitrogen. Tissue samples were collected from WT C57BL/6 mice and mice ($Kv4.2^{-/-}$ or $Kv4.3^{-/-}$) harboring targeted disruptions of the genes encoding Kv4.2 (*Kcnd2*) (35, 37) or Kv4.3 (*Kcnd3*) (45). Also, samples from mice ($Kv4.2^{-/-}$/$Kv4.3^{-/-}$) generated by crossing the $Kv4.2^{-/-}$ and $Kv4.3^{-/-}$ animals were used (46). Total protein samples from posterior cortices collected from adult WT, $Kv4.2^{-/-}$, $Kv4.2^{-/-}$, and $Kv4.3^{-/-}$/$Kv4.3^{-/-}$ mice were prepared using previously described methods (47).

The total protein content of each (HEK-293 cell and cortical) sample was quantified using the BCA protein assay kit (Pierce) prior to fractionation on SDS-PAGE gels. For Western blots, 45 μg (cortical) or 20 μg (HEK-293) of protein was loaded into each lane. Following fractionation, the proteins were transferred to PVDF membranes (Bio-Rad) and blocked with 5% nonfat dry milk in PBS with 0.1% Tween 20. The membranes were then incubated with a mouse monoclonal anti-Kv4.2 or anti-KChIP3 antibody or with a rabbit polyclonal anti-GFP (Millipore, Billerica, MA) or anti-DPP6 (48) antibody at 4 °C overnight. The anti-Kv4.2 and anti-KChIP3 antibodies were developed by and obtained from the UC Davis/National Institutes of Health NeuroMab facility, supported by National Institutes of Health Grant U24NS050606 and maintained by the University of California at Davis; the anti-DPP6 antibody was obtained from Dr. Bernardo Rudy. To ensure equal protein loading of lanes, membranes were also probed with a mouse monoclonal anti-transferrin receptor (Invitrogen) or a mouse monoclonal anti-GAPDH (Abcam, Cambridge, MA) antibody at room temperature for 1 h.

After washing, the membranes were incubated with a rabbit anti-mouse horseradish peroxidase-conjugated secondary antibody (Bethyl Laboratories, Montgomery, TX) or a donkey anti-rabbit horseradish peroxidase-conjugated secondary antibody (GE Healthcare Life Sciences) followed by SuperSignal West Dura extended duration substrate (Pierce). Signals were detected using a Molecular Imager Chemidoc XRS system running Quantity One software version 4.6 (Bio-Rad). For quantification, the signals corresponding to the anti-GAPDH (for DPP6) or anti-transferrin receptor (for Kv4.2, KChIP3, or GFP) antibodies were used to normalize the anti-DPP6, anti-Kv4.2, anti-GFP, or anti-KChIP3 signals as described in the text. The results are expressed as the means ± S.E. (4–11 experiments). Statistical differences between different groups were assessed using Student's *t* test.

*Immunoprecipitation of Kv4.2 Channel Subunits*—Immunoprecipitations were performed on cell lysates from HEK-293 cells co-transfected with KChIP3 or DPP6-YFP and WT or mutant Kv4.2 construct using 5 μg of a rabbit polyclonal anti-Kv4.2 antibody (Rbα Kv4.2; Sigma). Prior to immunoprecipitations, antibodies were cross-linked to 12.5 μl of protein A-magnetic beads (Invitrogen) using 20 mM dimethyl pimelimidate (Pierce). Protein samples and antibody-coupled beads were mixed for 2 h at 4 °C. Magnetic beads were then collected and washed rapidly four times with ice-cold lysis buffer, and isolated protein complexes were eluted from the beads in 1× SDS sample buffer. Purified cell surface proteins were then analyzed by Western blot as described above.

*Cell Surface Biotinylation*—Surface biotinylation of transfected HEK-293 cells was completed as previously described (44). Briefly, the cells were first incubated in $PBS_{MC}$ (PBS containing 1 mmol/liter $MgCl_2$, 0.1 mmol/liter $CaCl_2$) at 4 °C (to

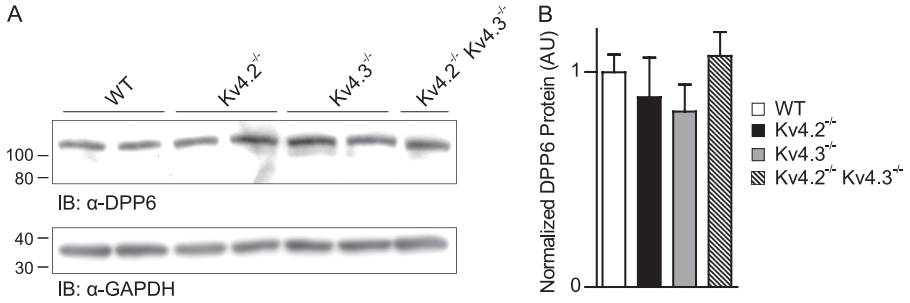


FIGURE 1. **Expression of DPP6 is unaffected by the targeted deletion of Kv4.2 and/or Kv4.3.** Representative Western blots (*A*) of fractionated total proteins prepared from posterior (~1 mm) cortices of WT, Kv4.2$^{-/-}$, Kv4.3$^{-/-}$, and Kv4.2$^{-/-}$/Kv4.3$^{-/-}$ mice. The intensities of the DPP6 bands were measured and normalized to the expression of the (endogenous) GAPDH in the same sample. The normalized DPP6 intensities in each Kv4.2$^{-/-}$, Kv4.3$^{-/-}$, or Kv4.2$^{-/-}$/Kv4.3$^{-/-}$ sample were then expressed relative to the average normalized DPP6 intensity in the WT samples. *B*, mean ± S.E. total DPP6 protein expression levels are similar in the cortices of WT ($n$ = 6), Kv4.2$^{-/-}$ ($n$ = 6), or Kv4.3$^{-/-}$ ($n$ = 6) animals, as well as animals lacking both Kv4.2$^{-/-}$ and Kv4.3$^{-/-}$ ($n$ = 4). *IB*, immunoblot.

inhibit membrane protein internalization) followed by $PBS_{MC}$ containing 0.25 mg/ml Sulfo-NHS-SS-Biotin (Pierce) for 30 min on ice. The biotinylation reaction was quenched with Tris-saline solution (10 mmol/liter Tris, pH 7.4, 120 mmol/liter NaCl, 1 mmol/liter $MgCl_2$, 0.1 mmol/liter $CaCl_2$), and the cells were washed with Tris-saline solution and collected. Detergent-soluble lysates were prepared, and biotinylated cell surface proteins were affinity-purified using NeutrAvidin-conjugated agarose beads (Pierce). Purified cell surface proteins were then subjected to Western blot analyses as described above.

## RESULTS

*Cortical DPP6 Expression Is Unaffected by Loss of Kv4.2 or Kv4.3*—Previous studies have documented the expression of DPP6 in brain and demonstrated that DPP6 immunoprecipitates with Kv4.2 from adult rat and mouse brain (14, 15, 48), consistent with suggestions that DPP6 is a component of native Kv4.2-encoded $I_A$ channel complexes (13, 30). Consistent with these findings and with a role for DPP6 in the generation of $I_A$ channels in cortical neurons, Western blot analysis revealed robust expression of DPP6 in wild type adult mouse visual cortex (Fig. 1). In addition, DPP6 expression in mouse cortex is unaffected by the targeted deletion of Kv4.2 and Kv4.3 (Fig. 1). Indeed, DPP6 protein expression levels in cortical lysates from mice lacking Kv4.2 (Kv4.2$^{-/-}$) or Kv4.3 (Kv4.3$^{-/-}$), as well as animals lacking both Kv4.2 and Kv4.3 (Kv4.2$^{-/-}$/Kv4.3$^{-/-}$), are indistinguishable from the expression level in wild type cortices (Fig. 1).

The observation that DPP6 expression is unaffected by the loss of Kv4.2 $\alpha$ subunits contrasts strikingly with recent findings demonstrating marked reductions in the expression of the accessory KChIP2, KChIP3, and KChIP4 subunits in Kv4.2$^{-/-}$ and Kv4.3$^{-/-}$ cortices and the virtual elimination of all three KChIP proteins in cortices from animals lacking both Kv4.2 and Kv4.3 (36), suggesting that different mechanisms underlie KChIP- and DPP-mediated increases in Kv4-encoded current densities (15, 17, 25, 26, 29, 31). Interestingly, consistent with this hypothesis, DPP6-YFP appears to be predominately localized at or near the plasma membrane when expressed (in HEK-293 cells) alone (Fig. 2*A*). Similar results are observed with DPP10-YFP (Fig. 2*B*), whereas KChIP3-YFP (Fig. 2*C*) is found diffusely in the cytosol (49). Cell surface labeling of unfixed DPP6-YFP-, DPP10-YFP-, and KChIP3-YFP-expressing cells was also performed with a polyclonal rabbit (IgG) antibody directed against GFP. The presence of YFP at the cell surface was visualized with an Alexa 555-tagged anti-rabbit IgG antibody (Fig. 2*D*). The fluorescence signals in the YFP and Alexa 555 channels overlap virtually completely (merged images are *yellow*) in the DPP6-YFP- and DPP10-YFP-expressing cells, whereas no Alexa 555 labeling was observed in KChIP3-YFP-expressing cells, and the merged image reveals only the green fluorescence from YFP. Line scans of YFP and Alexa 555 fluorescence intensities were obtained as described under "Experimental Procedures," and the means ± S.E. YFP intensities are plotted in the right panels of Fig. 2*D*. Consistent with the single cell images, the fluorescence intensity patterns are distinct, revealing plasma membrane localization for DPP6-YFP and DPP10-YFP and a diffuse cytosolic distribution for KChIP3-YFP.

*Co-expression with DPP6 Selectively Increases Cell Surface Kv4.2*—Although previous immunohistochemical studies have suggested that co-expression with DPP6 or DPP10 increases Kv4.2 protein at the cell surface (29, 33), it is unclear whether this reflects redistribution of existing Kv4.2 protein or, alternatively, a global increase in Kv4.2 protein expression. To address this question, total and cell surface Kv4.2 were examined in (HEK-293) cells expressing Kv4.2 in the absence and presence of DPP6. As illustrated in Fig. 3*A*, Western blot analyses revealed that total Kv4.2 expression levels were similar in cells co-expressing Kv4.2 with DPP6-YFP compared with cells expressing Kv4.2 alone. Cell surface Kv4.2 protein expression, however, was increased ~9-fold with DPP6-YFP co-expression (Fig. 3*B*, *right panel*). In marked contrast, neither total (Fig. 3*A*, *left panel*) nor cell surface (Fig. 3*B*, *left panel*) DPP6-YFP expression was measurably affected by Kv4.2 co-expression. These observations are consistent with the Western blot data on mouse cortices (Fig. 1), demonstrating that DPP6 expression is unaffected by the loss of Kv4.2 (and/or Kv4.3), as well as with the observation that DPP6 localizes to the cell surface in HEK-293 cells (Fig. 2) in the absence of Kv4 $\alpha$ subunits.

Additional experiments revealed that total Kv4.2 protein was also unaffected by the presence of DPP10-YFP (Fig. 4*A*, *right panel*). Also, similar to the results obtained with DPP6-YFP (Fig. 3), cell surface Kv4.2 protein expression was increased (~14-fold) with co-expression of DPP10-YFP (Fig. 4*A*, *right*

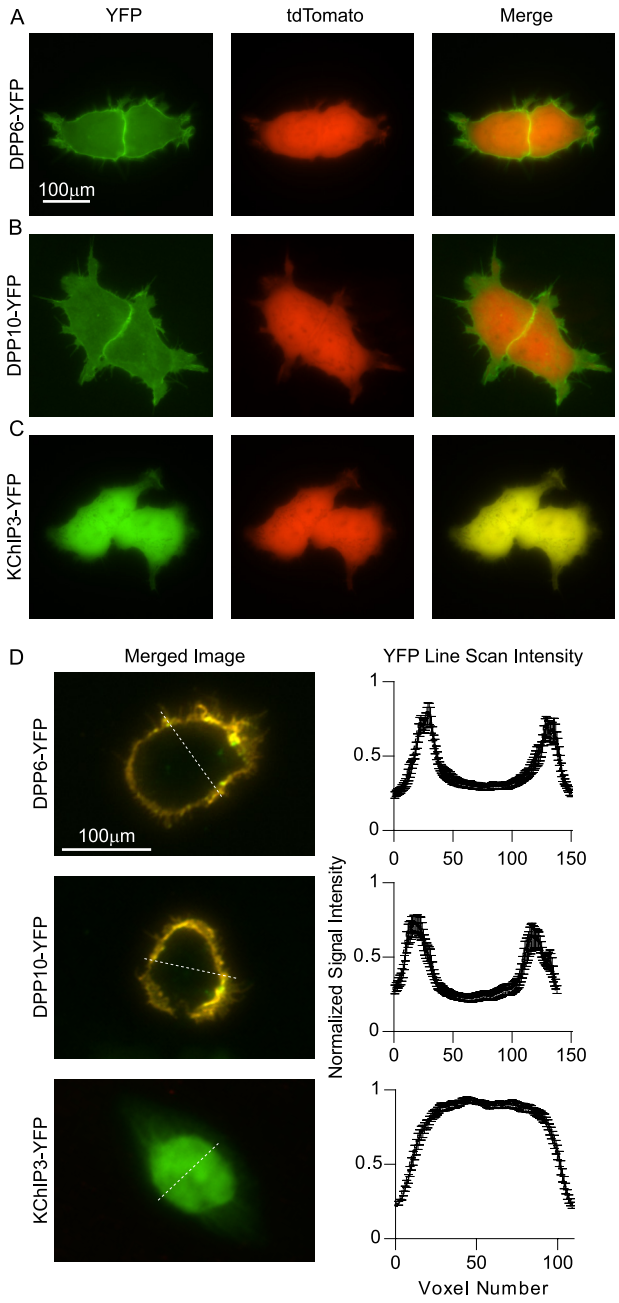


FIGURE 2. **DPP6 and DPP10 localize to the cell surface in the absence of Kv4 $\alpha$ subunits.** *A–C*, representative fluorescence images of HEK-293 cells transiently co-transfected with cDNA constructs encoding tdTomato and DPP6-YFP (*A*), DPP10-YFP (*B*), or KChIP3-YFP (*C*) are shown, with the *green* (*left*) and *red* (*middle*) channels depicted separately and merged (*right*). The DPP6-YFP and DPP10-YFP fluorescence is highest at or near the plasma membrane, whereas KChIP3-YFP fluorescence is diffuse throughout the cytosol. *D*, *left panels*, merged images of YFP and Alexa 555 fluorescence in cells transfected with DPP6-YFP (*top*), DPP10-YFP (*middle*), or KChIP3-YFP (*bottom*) in the absence of tdTomato following exposure to a polyclonal rabbit (IgG) anti-GFP antibody and an Alexa 555-conjugated goat anti-rabbit secondary antibody (see "Experimental Procedures"). The YFP and Alexa 555 signals overlap in DPP6-YFP-and DPP10-YFP-expressing cells and appear *yellow*, whereas no Alexa 555 staining was evident in the KChIP3-YFP-expressing cells, and only the green YFP fluorescence is observed. The mean ± S.E. line scan intensities of YFP fluorescence in DPP6-YFP-expressing ($n = 10$), DPP10-YFP-expressing ($n = 10$), and KChIP3-YFP-expressing ($n = 10$) cells illustrate the high plasma membrane expression of DPP6-YFP and DPP10-YFP compared with the cytosolic localization of KChIP3-YFP.

*panel*). Neither total (Fig. 4*A*, *left panel*) nor cell surface (Fig. 4*B*, *left panel*) DPP10-YFP expression, however, was measurably affected by Kv4.2. In contrast, co-expression with KChIP3 resulted in significant ($p < 0.001$) increases in both total (~2-fold) and cell surface (~15-fold) Kv4.2 protein expression, compared with cells expressing Kv4.2 alone (Fig. 4). As reported previously for KChIP2 (25, 49), the increase in total (and cell surface) Kv4.2 protein in the lysate likely reflects, at least in part, increased detergent solubility of Kv4.2. In addition, unlike DPP6 and DPP10, the KChIP3 protein was increased significantly ($p < 0.05$) in cells co-expressing Kv4.2 (Fig. 4*H*), consistent with mutual stabilization of the KChIP3 and Kv4.2 proteins (see "Discussion").

*Augmentation of Kv4.2 Currents by DPP6, DPP10, or KChIP3*—Heterologous expression of Kv4.2 alone reveals rapidly activating and inactivating outward Kv currents (24, 25, 49, 50). As reported previously (15, 30, 31), co-expression with DPP6-YFP ($p < 0.001$) or DPP10-YFP ($p < 0.001$) significantly increased Kv4.2 current densities (Fig. 3*E*). On average, Kv4.2 current densities were increased ~6-fold in cells transfected with equal amounts of Kv4.2 with DPP6-YFP or DPP10-YFP (Fig. 3*F*). Also consistent with previous findings (17, 26), co-expression with KChIP3 significantly ($p < 0.01$) increases Kv4.2 current densities (not illustrated).

The kinetics of Kv4.2 current inactivation are also affected by co-expression with DPP6-YFP, DPP10-YFP, or KChIP3 (17, 30, 31). The currents produced on heterologous expression of Kv4.2 alone in mammalian cell lines are best described by the sum of two exponentials that differ by approximately an order of magnitude (25, 50). The more rapidly inactivating component, with a mean ± S.E. ($n = 11$) time constant of inactivation ($\tau_{fast}$) of 13 ± 1 ms, contributed 83 ± 3% to the peak current at 0 mV. The inactivation time constant of the minor (17 ± 3%) more slowly inactivating component ($\tau_{slow}$) was 100 ± 9 ms. Co-expression with DPP6-YFP resulted in a significant ($p < 0.01$) reduction in the mean ± S.E. ($n = 12$) $\tau_{fast}$ (to 10 ± 1 ms) and an increase (to 94 ± 1%) in the fraction of the total current that inactivated rapidly (15, 30). Similar results were obtained with DPP10-YFP: mean ± S.E. ($n = 20$) $\tau_{fast}$ was reduced significantly ($p < 0.05$) to 11 ± 1 ms, and 89 ± 1% of total current inactivated rapidly.

In contrast to DPP6/10, the decay phases of the Kv4.2-encoded currents were dramatically prolonged in cells co-expressing KChIP3 (data not shown) reflecting an increase in the percentage of current that inactivates slowly rather than a change in the inactivation time constant (24, 26). Consistent with this suggestion, Kv4.2-encoded current inactivation in cells co-expressing KChIP3 was best characterized by a single exponential with a mean ± S.E. ($n = 5$) time constant of 79 ± 2 ms. Electrophysiological experiments conducted on cells co-expressing Kv4.2 with untagged DPP6, DPP10, or tagged KChIP3 (KChIP3-YFP) revealed Kv currents (data not shown) with properties indistinguishable from those recorded from cells co-expressing Kv4.2 with DPP6-YFP, DPP10-YFP, or (untagged) KChIP3 (Fig. 3), indicating that the presence of the YFP tags did not have any measurable effects on DPP6/10 or KChIP3 interactions with Kv4.2 $\alpha$ subunits or on Kv4.2-encoded currents.

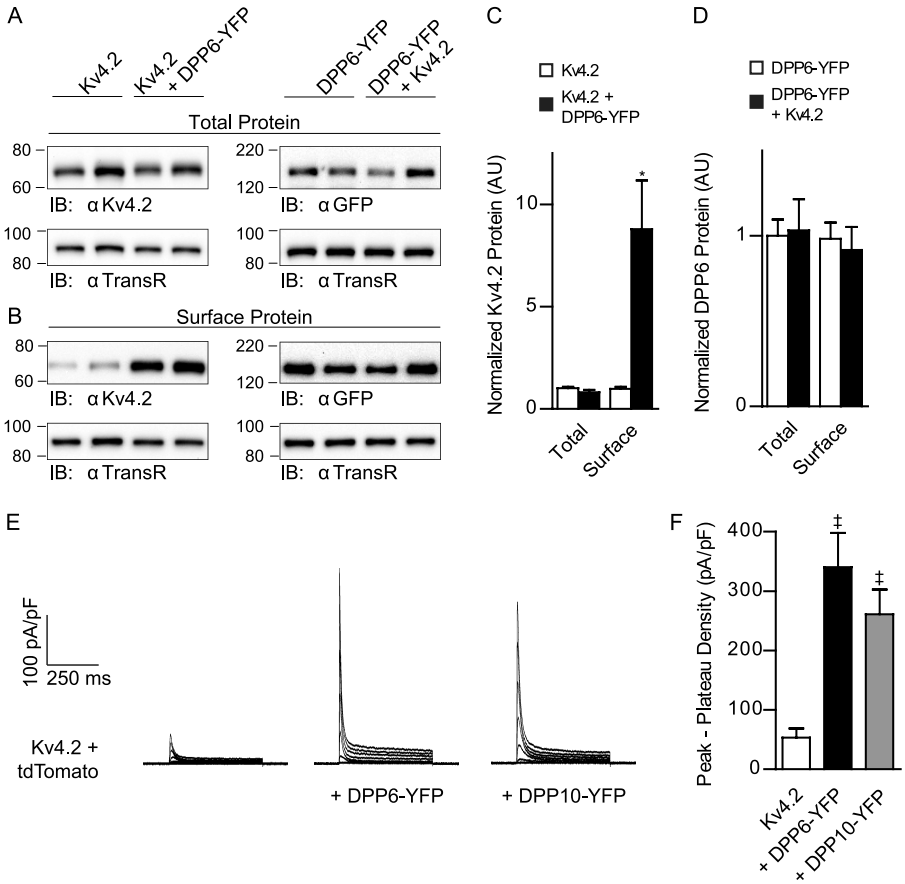


FIGURE 3. **DPP6 co-expression selectively increases cell surface Kv4.2 protein expression and Kv4.2-encoded current densities.** Total (*A*) and cell surface (*B*) proteins prepared from HEK-293 cells transiently transfected with cDNA constructs encoding Kv4.2, DPP6-YFP, or both Kv4.2 and DPP6-YFP were fractionated on SDS-PAGE gels and probed with anti-Kv4.2 (*left*) and anti-GFP (*right*) antibodies, as well as with an anti-transferrin receptor antibody. The intensities of each of the Kv4.2 bands were measured and normalized to the expression of the (endogenous) transferrin receptor in the same sample. The normalized Kv4.2 band intensities in the samples in which DPP6-YFP was co-expressed were then compared with the average normalized Kv4.2 intensity measured in the samples from cells expressing Kv4.2 alone. Mean ± S.E. ($n = 6$ samples) total (*A*) and cell surface (*B*) Kv4.2 protein expression levels in cells expressing Kv4.2 in the absence and in the presence of DPP6-YFP are plotted (*C*). The intensities of the anti-GFP bands (reflecting the expression of YFP-tagged DPP6) were similarly normalized, and mean ± S.E. ($n = 6$) total (*A*) and cell surface (*B*) DPP6-YFP protein expression levels in cells expressing DPP6-YFP in the absence and in the presence of Kv4.2 are plotted in *D*. As is evident, cell surface, but not total, Kv4.2 protein expression was increased significantly (*, $p < 0.05$) with DPP6-YFP co-expression (*C*). Total and cell surface DPP6-YFP protein expression, in contrast, were not measurably affected by the presence of Kv4.2 (*D*). Whole cell outward $K^+$ currents, evoked in response to depolarizing voltage steps to potentials between −60 and +40 mV (in 10-mV increments) from a holding potential of −70 mV, were recorded from HEK-293 cells transiently transfected with cDNA constructs encoding tdTomato with Kv4.2 in the absence and in the presence of DPP6-YFP or DPP10-YFP. Representative records are shown in *E*, and mean ± S.E. ($n = 13$–20) (peak-plateau) $K^+$ current densities (at 0 mV) are presented in *F*. Rapidly activating and inactivating $K^+$ currents were routinely observed in cells expressing Kv4.2, and current densities were increased significantly with DPP6-YFP or DPP10-YFP co-expression (see text). ‡, values indicated are significantly different from Kv4.2 current densities in cells expressing Kv4.2 alone at the $p < 0.001$ level. *IB*, immunoblot.

*Role for Kv4.2 N Terminus in DPP-mediated Regulation of Kv4 Currents*—Several previous studies have suggested a role for the distal Kv4 N terminus in regulating the inactivation of Kv4-encoded currents (24, 25, 50). It has also been reported that co-expression of Kv4.2 with a novel N-terminal DPP6 splice variant alters the kinetics of Kv4.2 current inactivation (51). Together, these results suggest a role for the Kv4.2 N terminus in mediating the functional effects of DPP6/10. To explore this hypothesis, whole cell $K^+$ currents were recorded from cells expressing the Kv4.2 N-terminal deletion mutant, Kv4.2Δ40N (24, 25, 50). As reported previously, peak current densities were (~4-fold) higher in cells expressing Kv4.2Δ40N (25), compared with cells expressing WT Kv4.2 (Fig. 5*A*). Analyses of the decay phases of the currents also revealed that both components of inactivation were slowed with N-terminal deletion (compared with WT Kv4.2) and that only 34 ± 4% of the peak Kv4.2Δ40N current inactivated rapidly (24, 25).

Co-expression with DPP6-YFP increased Kv4.2Δ40N-encoded currents significantly ($p < 0.05$), although the magnitude of the increase (~2-fold) was smaller than the ~6-fold increase observed for WT Kv4.2 (Fig. 5*B*). Additionally, the marked slowing of Kv4.2 current inactivation that is evident in cells expressing Kv4.2Δ40N was not overcome by co-expression of DPP6-YFP (Fig. 5*A*). Biochemical experiments revealed that co-expression with DPP6-YFP selectively increased cell surface Kv4.2Δ40N protein expression (Fig. 5*D*) similar to WT Kv4.2. The (3-fold) magnitude of the increase, however, was substantially less than the (~9-fold) increase in cell surface WT Kv4.2 protein with co-expression of DPP6-YFP. Similar to WT Kv4.2, however, total Kv4.2Δ40N protein was unaffected by DPP6-YFP co-expression (Fig. 5*C*). Further biochemical experiments demonstrated that, in contrast to KChIP3, DPP6-YFP co-immunoprecipitated efficiently with a C-terminal anti-K4.2 antibody from cells co-expressing Kv4.2D40N and DPP6-YFP (Fig.

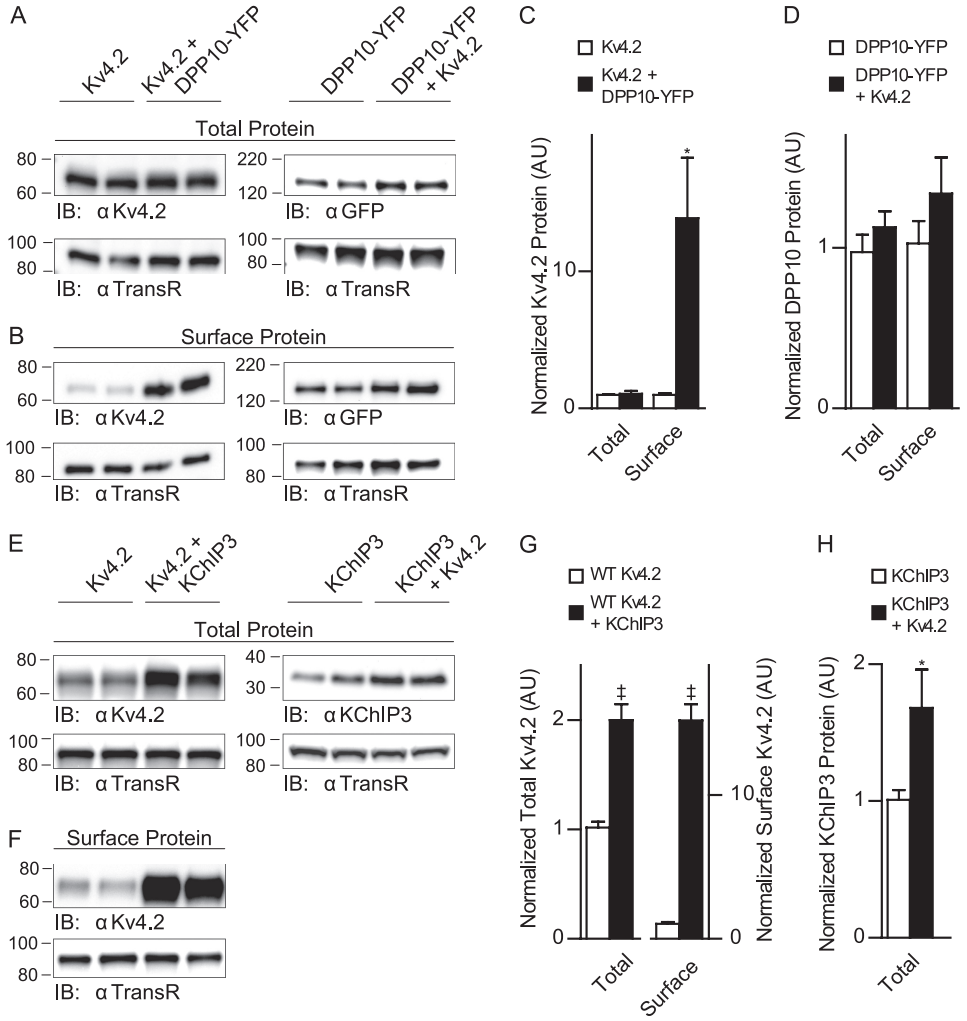


FIGURE 4. **Co-expression with DPP10 also selectively increases cell surface Kv4.2 protein expression, whereas total and cell surface Kv4.2 are increased with KChIP3 co-expression.** Representative Western blots of fractionated total (*A* and *E*) and cell surface (*B* and *F*) proteins from HEK-293 cells transiently transfected with cDNA constructs encoding Kv4.2 alone, Kv4.2 + DPP10-YFP, DPP10-YFP alone, KChIP3 alone, or Kv4.2 + KChIP3. In each experiment, the intensities of the Kv4.2, DPP10-YFP, and KChIP3 bands were measured and normalized as described in the legend to Fig. 3. Mean ± S.E. total and cell surface Kv4.2 in cells expressing Kv4.2 alone and in the presence of DPP10-YFP ($n = 8$) (*C*) or KChIP3 ($n = 6$) (*G*) are plotted. Similarly, mean ± S.E. total and cell surface DPP10-YFP and KChIP3 in cells expressing DPP10-YFP ($n = 11$) (*D*) or KChIP3 ($n = 10$) (*H*) alone and in the presence of Kv4.2 are presented. Similar to the findings with DPP6 (Fig. 3), cell surface, but not total, Kv4.2 protein expression was increased significantly (*, $p < 0.05$) with DPP10-YFP co-expression (*C*). In contrast, co-expression with KChIP3 resulted in significant (‡, $p < 0.001$) increases in both total and cell surface Kv4.2 protein expression. In addition, although neither total nor cell surface DPP10-YFP was affected by Kv4.2 co-expression (*D*), KChIP3 protein expression was increased significantly (*, $p < 0.05$) in the presence of Kv4.2 (*H*). *IB*, immunoblot.

5*G*), suggesting that the observed differences in the magnitude of the DPP6-mediated increases in current densities (Fig. 5*B*) and cell surface protein (Fig. 5*E*) in cells expressing Kv4.2Δ40N, compared with WT Kv4.2, do not reflect decreased Kv4.2/DPP6 binding affinity.

*DPP10 and KChIP3 Promote Kv4.2 Expression through Independent Mechanisms*—Previous studies have suggested that native $I_A$ channel complexes reflect the trimeric co-assembly of Kv4 $\alpha$ subunits with KChIP and DPP accessory subunits (31, 51). Interestingly, Western blot analyses revealed that the co-expression of KChIP3 with Kv4.2 and DPP10 resulted in a further (~12-fold) increase in cell surface Kv4.2 protein expression compared with cells expressing Kv4.2 and DPP10-YFP (Fig. 6*B*). Similar to results obtained in the absence of DPP10-YFP, KChIP3 also significantly (#, $p < 0.01$) increased total Kv4.2 protein expression (~2-fold) in cells expressing Kv4.2 and DPP10-YFP. The magnitudes of increases in total and cell surface Kv4.2 protein were similar to those observed with KChIP3 co-expression in the absence of DPP10-YFP, suggesting that the KChIP3 and DPP6/DPP10 accessory subunits independently regulate Kv4 protein expression (see "Discussion").

## DISCUSSION

*DPP6/10 Protein Stability and Subcellular Localization Are Independent of Kv4.2*—The results presented here demonstrate that the expression of DPP6 in adult mouse cortex is unaffected by the targeted deletion of the Kv4.2 and/or Kv4.3 $\alpha$ subunits. These observations are in striking contrast to previous studies demonstrating marked decreases in the expression of KChIP2, KChIP3, and KChIP4 in the cortices of animals lacking either Kv4.2 or Kv4.3 and nearly complete loss of all three KChIP proteins with the elimination of both Kv4.2 and Kv4.3 (36), suggesting that distinct mechanisms underlie DPP6- and KChIP-mediated regulation of Kv4 currents. Consistent with

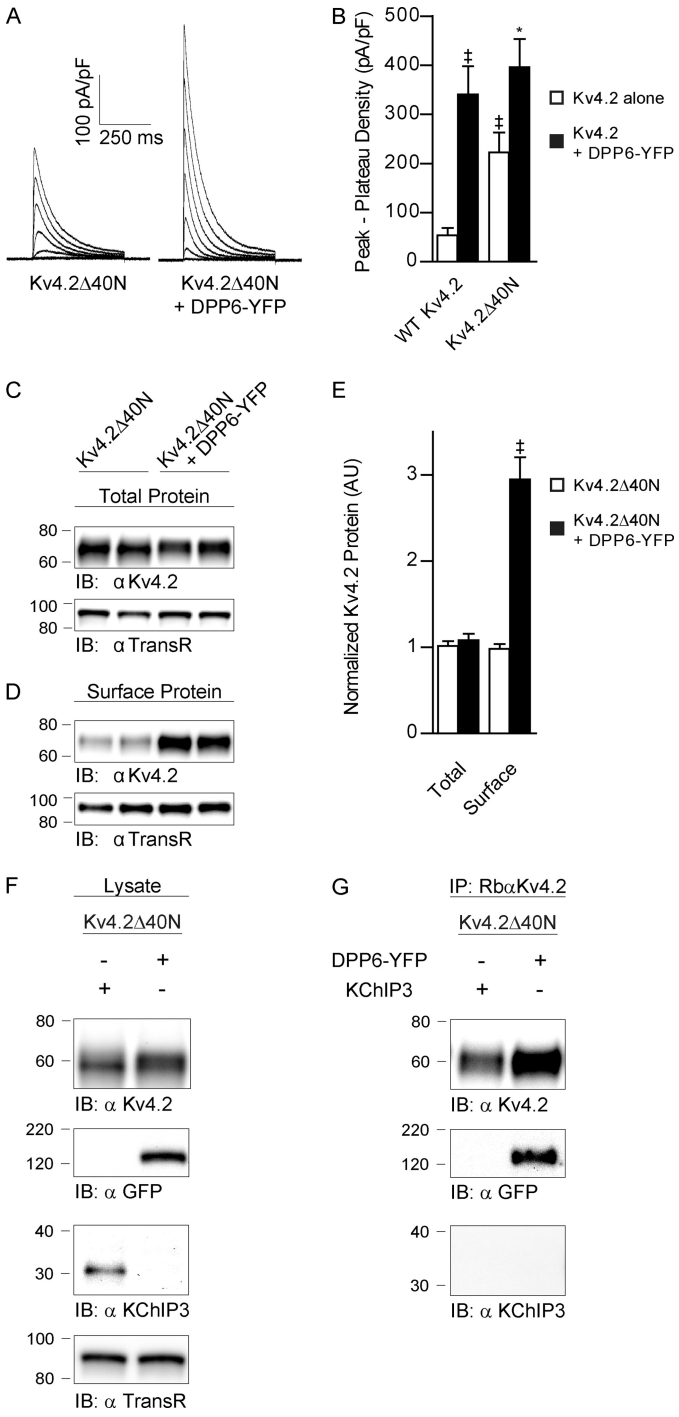


FIGURE 5. **Kv4.2 N-terminal deletion reduces DPP6-mediated effects on Kv4.2 protein and currents.** Whole cell outward $K^+$ currents were recorded as described in the legend to Fig. 3 from HEK-293 cells transiently transfected with cDNA constructs encoding tdTomato together with the Kv4.2 N-terminal deletion mutant, Kv4.2Δ40N, in the absence and in the presence of DPP6-YFP. Representative records are shown in *A*, and mean ± S.E. $K^+$ current densities ($n = 19–21$), measured at 0 mV, are plotted in *B*. Mean ± S.E. $K^+$ current densities in cells expressing full-length WT Kv4.2 in the absence and in the presence of DPP6-YFP are replotted from Fig. 3*F* for comparison. As reported previously (24, 25), whole cell $K^+$ current amplitudes/densities were significantly (‡, $p < 0.001$) higher in cells expressing Kv4.2Δ40N compared with cells expressing WT Kv4.2 (*B*). Co-expression of DPP6-YFP with Kv4.2Δ40N resulted in a ~2-fold increase in $K^+$ current densities. Representative Western blots of fractionated total (*C*) and cell surface (*D*) proteins prepared from HEK-293 cells transiently transfected with cDNA constructs encoding Kv4.2Δ40N in the absence and in the presence of DPP6-YFP are also illustrated. The intensities of the Kv4.2 bands were normalized as described in the legend to Fig. 3, and mean ± S.E. total (*A*) and cell surface (*B*) Kv4.2Δ40N protein levels in cells expressing Kv4.2Δ40N alone or with DPP6-YFP ($n = 6$) are presented in *E*. Similar to WT Kv4.2, cell surface, but not total, Kv4.2Δ40N protein expression was increased significantly (‡, $p < 0.001$) with DPP6-YFP co-expression (*E*), although the magnitude (~3-fold) of the increase was less than the ~9-fold increase seen with WT Kv4.2 (Fig. 3). Lysates from HEK-293 cells co-transfected with Kv4.2Δ40N and either DPP6-YFP or KChIP3 were immunoprecipitated with a rabbit anti-Kv4.2 antibody directed against the C terminus of Kv4.2. Representative Western blots of the cell lysates before immunoprecipitation (*F*) and of immunoprecipitated proteins (*G*) revealed that, in contrast to KChIP3, DPP6-YFP was efficiently co-immunoprecipitated with Kv4.2Δ40N (*G*). *IB*, immunoblot.

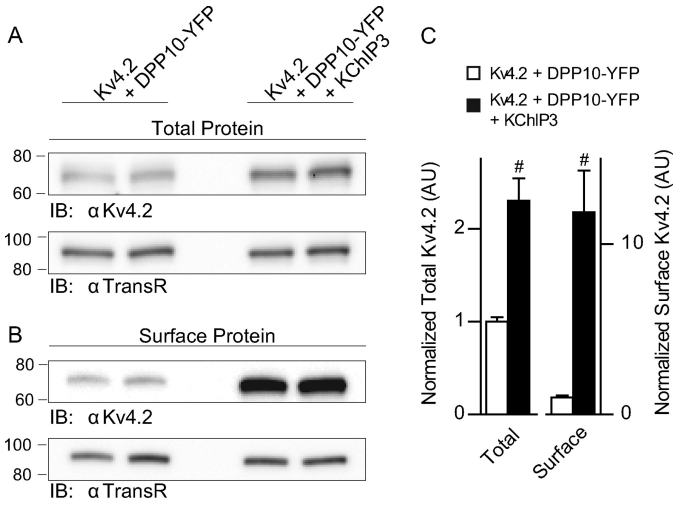


FIGURE 6. **KChIP3 increases total and cell surface Kv4.2 protein in the presence of DPP10.** Representative Western blots of fractionated total (*A*) and cell surface (*B*) proteins prepared from HEK-293 cells transiently transfected with cDNA constructs encoding Kv4.2 and DPP10-YFP in the absence (*left*) and in the presence (*right*) of KChIP3. The intensities of the Kv4.2 bands were measured and normalized as described in the legend to Fig. 3. Mean ± S.E. total and cell surface Kv4.2 protein expression levels in cells co-expressing Kv4.2 and DPP10-YFP in the absence ($n = 6$) and in the presence ($n = 6$) of KChIP3 are plotted in *C*. The addition of KChIP3 resulted in significant (#, $p < 0.01$) increases in both total and cell surface Kv4.2 protein expression compared with cells expressing DPP10-YFP, and the magnitudes of these increases were similar to those produced in the absence of DPP10 or DPP6 (see text). *IB*, immunoblot.

this suggestion, DPP6 and DPP10 traffic efficiently to the cell surface in the absence of Kv4 α subunits (Fig. 2), whereas the KChIPs are diffusely cytosolic (17, 49) and only localize to the cell surface when co-expressed with Kv4 α subunits (52).

The biochemical experiments here (Figs. 3 and 4) also demonstrate that the stabilities of the DPP6 and DPP10 proteins do not depend on Kv4.2 expression, results consistent with the findings in the cortex (Fig. 1). In addition, the observation that the cell surface expression of DPP6 and DPP10 was unaffected by the presence of Kv4.2 suggests not only that the DPP6 and DPP10 subunits traffic to the surface membrane independent of Kv4.2, but also that there is no subcellular redistribution of the DPP6/10 subunits with Kv4.2 co-expression. In contrast, KChIP3 protein expression was increased significantly in the presence of Kv4.2, consistent with previous findings for KChIP2 (25, 36) and with the suggestion that association with Kv4 α subunits results in the stabilization of KChIP3. Also similar to the results with KChIP2, the association of KChIP3 with Kv4.2 subunits stabilizes the Kv4.2 protein and increases the localization of Kv4.2-KChIP3 channel complexes at the cell surface.

*Molecular Determinants of Kv4.2/DPP6 Interactions*—The biochemical experiments here demonstrate that, in contrast to the KChIPs (24, 25), the distal N terminus of Kv4.2 is not required for Kv4.2/DPP6 protein-protein interactions (Fig. 5G). Deletion of the distal Kv4.2 N terminus, however, resulted in a smaller (~3-fold) increase in cell surface Kv4.2Δ40N protein expression compared with (~9-fold) increases observed with WT Kv4.2. DPP6-mediated (~2-fold) increases in Kv4.2Δ40N current densities were also considerably smaller than the (~6-fold) increases in WT Kv4.2 current densities in the presence of DPP6. In addition, in marked contrast with WT Kv4.2, expression of DPP6 with Kv4.2Δ40N did not result in accelerated inactivation. Taken together, these results suggest a role for the Kv4.2 N terminus in mediating the effects of DPP6 on Kv4.2 cell surface protein expression and current densities but also suggest that domains, in addition to the N terminus, are also involved.

Previous biochemical studies, exploiting Kv4.3/Kv1.4 chimeric constructs, suggested a critical role for the second transmembrane (S2) domain in Kv4.3 in mediating the interaction with DPP10 (53). Mutational analysis of residues in the S2 domain further suggested a critical role for the alanine residue at position 232 in Kv4.3 as changing alanine 232 to valine reportedly reduced Kv4.3 association with DPP10 by >80% (53). It was also reported that co-expression of DPP10 with Kv4.3A232V did not measurably accelerate the kinetics of Kv4.3 current inactivation, although current waveforms were not presented, and the impact of the A232V mutation on Kv4.3 current densities in the absence or presence of DPP10 was not described (53). Additional experiments here, designed to quantify the role of the homologous alanine residue in the Kv4.2 S2 domain (supplemental Fig. S1*A*) in mediating the effects of DPP6/10 on Kv4.2 protein expression and current densities, however, revealed that whole cell $K^+$ current waveforms in cells expressing Kv4.2A235V (supplemental Fig. S1*B*) were indistinguishable from those measured in cells expressing WT Kv4.2 (Fig. 3*E*).

In addition, similar to WT Kv4.2 (Fig. 3*E*), DPP6-YFP co-expression markedly accelerated current inactivation (supplemental Fig. 1*B*), and $K^+$ current densities were increased ~6-fold (supplemental Fig. 1*C*). Also, similar to WT Kv4.2, current inactivation was accelerated in the presence of DPP6-YFP. Parallel biochemical experiments revealed that DPP6-YFP co-expression selectively increased cell surface (supplemental Fig. 1*F*), without measurably affecting total (supplemental Fig. 1*E*) Kv4.2A235V protein expression, and the magnitude of the increase was similar to that observed in cells co-expressing DPP6-YFP with WT Kv4.2 (Fig. 3*C*). Taken together, these results clearly suggest that Ala-235 is not a critical residue involved in DPP-mediated regulation of Kv4.2 currents. Further experiments, designed to probe the functional roles of additional residues in the S2 domain (53), as well perhaps as S1 and the proximal N terminus, are needed to define the critical domains/residues in Kv4.2 that mediate interactions with DPP6/10.

*DPP6 and DPP10 Selectively Increase Cell Surface Kv4.2 Protein Expression*—In addition to increasing the rate of Kv4.2 current inactivation, co-expression with either DPP6 or DPP10 markedly increases current densities (15, 16, 29–31). Although a ~2-fold (from 4 to 7.5 pS) increase in the unitary conductance of Kv4.2-encoded channels has been offered as one mechanism whereby DPP subunits increase Kv4.2 current amplitudes/densities (32), the biochemical data presented here demonstrate that DPP6 and DPP10 selectively stabilize the Kv4.2 protein at the cell surface by ~10-fold, which would be expected to contribute importantly to increasing macroscopic neuronal Kv4.2-encoded current densities. Taken together with the observation that DPP6 and DPP10 autonomously traffic to the cell surface, it seems reasonable to suggest that DPP subunits do not promote forward trafficking of assembled (Kv4.2/KChIP3) channel complexes but rather act to selectively stabilize Kv4.2-encoded channels at the cell surface. It is tempting to speculate, therefore, that there may exist, in neurons, distinct populations of Kv4-encoded channels, those with and those without DPP subunits.

In contrast with DPP6/10, co-expression with KChIP3 stabilizes both total and cell surface Kv4.2 protein, as well as being reciprocally stabilized in the presence of Kv4.2 (25, 36, 38, 39). These results are similar to previous findings with KChIP2, consistent with similar functional roles for the KChIP2 and KChIP3 proteins (25, 33). It seems reasonable to suggest that early association between the Kv4 and KChIP subunits is required (and is maintained) for enhanced K4-KChIP complex stability. Interestingly, previous experiments have revealed that the association of T-type voltage-gated $Ca^{2+}$ (Cav) channels together with Kv4.2/KChIP3/DPP10 channels results in macromolecular signaling complexes (54, 55). This association results in calcium-dependent regulation of Kv4.2-encoded channels and requires the presence of KChIP3 but not DPP10.

Importantly, the addition of KChIP3 in the presence of DPP10 results in further increases (~10-fold) in cell surface Kv4.2 protein (Fig. 6), revealing that the presence of DPP accessory subunits does not exclude interactions with the KChIPs and further that the KChIP and DPP subunits independently stabilize cell surface Kv4.2 protein and increase the functional cell surface expression of Kv4-encoded macromolecular channel complexes.

*Acknowledgments—We thank Dr. Bernardo Rudy for the gift of the DPP6 antibody, Rebecca Mellor for assistance with the generation of plasmids, and Rick Wilson for the maintenance and screening of the mouse lines used in this study. We also thank Drs. Kai-Chien Yang and Yarimar Carrasquillo for many valuable discussions and for comments on the manuscript.*

## REFERENCES

1. Segal, M., Rogawski, M. A., and Barker, J. (1984) A transient potassium conductance regulates the excitability of cultured hippocampal and spinal neurons. *J. Neurosci.* **4,** 604–609
2. Rogawski, M. A. (1985) The A-current: how ubiquitous a feature of excitable cells is it? *Trends Neurosci.* **8,** 214–219
3. Kim, J., Wei, D. S., and Hoffman, D. A. (2005) Kv4 potassium channel subunits control action potential repolarization and frequency-dependent broadening in rat hippocampal CA1 pyramidal neurones. *J. Physiol.* **569,** 41–57
4. Kang, J., Huguenard, J. R., and Prince, D. A. (2000) Voltage-gated potassium channels activated during action potentials in layer V neocortical

pyramidal neurons. *J. Neurophysiol.* **83,** 70–80
5. Bekkers, J. M. (2000) Distribution and activation of voltage-gated potassium channels in cell-attached and outside-out patches from large layer 5 cortical pyramidal neurons of the rat. *J. Physiol.* **525,** 611–620
6. Birnbaum, S. G., Varga, A. W., Yuan, L. L., Anderson, A. E., Sweatt, J. D., and Schrader, L. A. (2004) Structure and function of Kv4-family transient potassium channels. *Physiol. Rev.* **84,** 803–833
7. Yuan, W., Burkhalter, A., and Nerbonne, J. M. (2005) Functional role of the fast transient outward $K^+$ current IA in pyramidal neurons in (rat) primary visual cortex. *J. Neurosci.* **25,** 9185–9194
8. Connor, J. A., and Stevens, C. F. (1971) Voltage clamp studies of a transient outward membrane current in gastropod neural somata. *J. Physiol.* **213,** 21–30
9. Cai, X., Liang, C. W., Muralidharan, S., Kao, J. P., Tang, C. M., and Thompson, S. M. (2004) Unique roles of SK and Kv4.2 potassium channels in dendritic integration. *Neuron* **44,** 351–364
10. Hoffman, D. A., Magee, J. C., Colbert, C. M., and Johnston, D. (1997) $K^+$ channel regulation of signal propagation in dendrites of hippocampal pyramidal neurons. *Nature* **387,** 869–875
11. Stuart, G., Spruston, N., Sakmann, B., and Häusser, M. (1997) Action potential initiation and backpropagation in neurons of the mammalian CNS. *Trends Neurosci.* **20,** 125–131
12. Häusser, M., Spruston, N., and Stuart, G. J. (2000) Diversity and dynamics of dendritic signaling. *Science* **290,** 739–744
13. Maffie, J., and Rudy, B. (2008) Weighing the evidence for a ternary protein complex mediating A-type K+ currents in neurons. *J. Physiol.* **586,** 5609–5623
14. Marionneau, C., LeDuc, R. D., Rohrs, H. W., Link, A. J., Townsend, R. R., and Nerbonne, J. M. (2009) Proteomic analyses of native brain $K_V4.2$ channel complexes. *Channels* **3,** 284–294
15. Nadal, M. S., Ozaita, A., Amarillo, Y., Vega-Saenzde Miera, E., Ma, Y., Mo, W., Goldberg, E. M., Misumi, Y., Ikehara, Y., Neubert, T. A., and Rudy, B. (2003) The CD26-related dipeptidyl aminopeptidase-like protein DPPX is a critical component of neuronal A-type $K^+$ channels. *Neuron* **37,** 449–461
16. Jerng, H. H., Qian, Y., and Pfaffinger, P. J. (2004) Modulation of Kv4.2 channel expression and gating by dipeptidyl peptidase 10 (DPP10). *Biophys. J.* **87,** 2380–2396
17. An, W. F., Bowlby, M. R., Betty, M., Cao, J., Ling, H. P., Mendoza, G., Hinson, J. W., Mattsson, K. I., Strassle, B. W., Trimmer, J. S., and Rhodes, K. J. (2000) Modulation of A-type potassium channels by a family of calcium sensors. *Nature* **403,** 553–556
18. Petrecca, K., Miller, D. M., and Shrier, A. (2000) Localization and enhanced current density of the Kv4.2 potassium channel by interaction with the actin-binding protein filamin. *J. Neurosci.* **20,** 8736–8744
19. Gardoni, F., Mauceri, D., Marcello, E., Sala, C., Di Luca, M., and Jeromin, A. (2007) SAP97 directs the localization of Kv4.2 to spines in hippocampal neurons. Regulation by CaMKII. *J. Biol. Chem.* **282,** 28691–28699
20. Marshall, C. R., Noor, A., Vincent, J. B., Lionel, A. C., Feuk, L., Skaug, J., Shago, M., Moessner, R., Pinto, D., Ren, Y., Thiruvahindrapduram, B., Fiebig, A., Schreiber, S., Friedman, J., Ketelaars, C. E., Vos, Y. J., Ficicioglu, C., Kirkpatrick, S., Nicolson, R., Sloman, L., Summers, A., Gibbons, C. A., Teebi, A., Chitayat, D., Weksberg, R., Thompson, A., Vardy, C., Crosbie, V., Luscombe, S., Baatjes, R., Zwaigenbaum, L., Roberts, W., Fernandez, B., Szatmari, P., and Scherer, S. W. (2008) Structural variation of chromosomes in autism spectrum disorder. *Am. J. Hum. Genet.* **82,** 477–488
21. Cronin, S., Berger, S., Ding, J., Schymick, J. C., Washecka, N., Hernandez, D. G., Greenway, M. J., Bradley, D. G., Traynor, B. J., and Hardiman, O. (2008) A genome-wide association study of sporadic ALS in a homogenous Irish population. *Hum. Mol. Genet.* **17,** 768–774
22. van Es, M. A., van Vught, P. W., Blauw, H. M., Franke, L., Saris, C. G., Van den Bosch, L., de Jong, S. W., de Jong, V., Baas, F., van't Slot, R., Lemmens, R., Schelhaas, H. J., Birve, A., Sleegers, K., Van Broeckhoven, C., Schymick, J. C., Traynor, B. J., Wokke, J. H., Wijmenga, C., Robberecht, W., Andersen, P. M., Veldink, J. H., Ophoff, R. A., and van den Berg, L. H. (2008) Genetic variation in DPP6 is associated with susceptibility to amyotrophic lateral sclerosis. *Nat. Genet.* **40,** 29–31
23. Burgoyne, R. D., and Weiss, J. L. (2001) The neuronal calcium sensor family of $Ca^{2+}$-binding proteins. *Biochem. J.* **353,** 1–12
24. Bähring, R., Dannenberg, J., Peters, H. C., Leicher, T., Pongs, O., and Isbrandt, D. (2001) Conserved Kv4 N-terminal domain critical for effects of Kv channel-interacting protein 2.2 on channel expression and gating. *J. Biol. Chem.* **276,** 23888–23894
25. Foeger, N. C., Marionneau, C., and Nerbonne, J. M. (2010) Co-assembly of Kv4 $\alpha$ subunits with K+ channel-interacting protein 2 stabilizes protein expression and promotes surface retention of channel complexes. *J. Biol. Chem.* **285,** 33413–33422
26. Kunjilwar, K., Strang, C., DeRubeis, D., and Pfaffinger, P. J. (2004) KChIP3 rescues the functional expression of Shal channel tetramerization mutants. *J. Biol. Chem.* **279,** 54542–54551
27. Kin, Y., Misumi, Y., and Ikehara, Y. (2001) Biosynthesis and characterization of the brain-specific membrane protein DPPX, a dipeptidyl peptidase IV-related protein. *J. Biochem.* **129,** 289–295
28. Strop, P., Bankovich, A. J., Hansen, K. C., Garcia, K. C., and Brunger, A. T. (2004) Structure of a human A-type potassium channel interacting protein DPPX, a member of the dipeptidyl aminopeptidase family. *J. Mol. Biol.* **343,** 1055–1065
29. Zagha, E., Ozaita, A., Chang, S. Y., Nadal, M. S., Lin, U., Saganich, M. J., McCormack, T., Akinsanya, K. O., Qi, S. Y., and Rudy, B. (2005) DPP10 modulates Kv4-mediated A-type potassium channels. *J. Biol. Chem.* **280,** 18853–18861
30. Amarillo, Y., De Santiago-Castillo, J. A., Dougherty, K., Maffie, J., Kwon, E., Covarrubias, M., and Rudy, B. (2008) Ternary Kv4.2 channels recapitulate voltage-dependent inactivation kinetics of A-type $K^+$ channels in cerebellar granule neurons. *J. Physiol.* **586,** 2093–2106
31. Jerng, H. H., Kunjilwar, K., and Pfaffinger, P. J. (2005) Multiprotein assembly of Kv4.2, KChIP3 and DPP10 produces ternary channel complexes with ISA-like properties. *J. Physiol.* **568,** 767–788
32. Kaulin, Y. A., De Santiago-Castillo, J. A., Rocha, C. A., Nadal, M. S., Rudy, B., and Covarrubias, M. (2009) The dipeptidyl-peptidase-like protein DPP6 determines the unitary conductance of neuronal Kv4.2 channels. *J. Neurosci.* **29,** 3242–3251
33. Seikel, E., and Trimmer, J. S. (2009) Convergent modulation of Kv4.2 channel $\alpha$ subunits by structurally distinct DPPX and KChIP auxiliary subunits. *Biochemistry* **48,** 5721–5730
34. Sun, W., Maffie, J. K., Lin, L., Petralia, R. S., Rudy, B., and Hoffman, D. A. (2011) DPP6 establishes the A-type $K^+$ current gradient critical for the regulation of dendritic excitability in CA1 hippocampal neurons. *Neuron* **71,** 1102–1115
35. Guo, W., Jung, W. E., Marionneau, C., Aimond, F., Xu, H., Yamada, K. A., Schwarz, T. L., Demolombe, S., and Nerbonne, J. M. (2005) Targeted deletion of Kv4.2 eliminates I(to,f) and results in electrical and molecular remodeling, with no evidence of ventricular hypertrophy or myocardial dysfunction. *Circ. Res.* **97,** 1342–1350
36. Norris, A. J., Foeger, N. C., and Nerbonne, J. M. (2010) Interdependent roles for accessory KChIP2, KChIP3, and KChIP4 subunits in the generation of Kv4-encoded IA channels in cortical pyramidal neurons. *J. Neurosci.* **30,** 13644–13655
37. Nerbonne, J. M., Gerber, B. R., Norris, A., and Burkhalter, A. (2008) Electrical remodelling maintains firing properties in cortical pyramidal neurons lacking KCND2-encoded A-type K+ currents. *J. Physiol.* **586,** 1565–1579
38. Chen, X., Yuan, L. L., Zhao, C., Birnbaum, S. G., Frick, A., Jung, W. E., Schwarz, T. L., Sweatt, J. D., and Johnston, D. (2006) Deletion of Kv4.2 gene eliminates dendritic A-type K+ current and enhances induction of long-term potentiation in hippocampal CA1 pyramidal neurons. *J. Neurosci.* **26,** 12143–12151
39. Menegola, M., and Trimmer, J. S. (2006) Unanticipated region- and cell-specific downregulation of individual KChIP auxiliary subunit isotypes in Kv4.2 knock-out mouse brain. *J. Neurosci.* **26,** 12137–12142
40. Wu, M. N., Joiner, W. J., Dean, T., Yue, Z., Smith, C. J., Chen, D., Hoshi, T., Sehgal, A., and Koh, K. (2010) SLEEPLESS, a Ly-6/neurotoxin family member, regulates the levels, localization and activity of Shaker. *Nat. Neurosci.* **13,** 69–75
41. Johns, D. C., Marx, R., Mains, R. E., O'Rourke, B., and Marbán, E. (1999) Inducible genetic suppression of neuronal excitability. *J. Neurosci.* **19,**

1691–1697
42. Shaner, N. C., Campbell, R. E., Steinbach, P. A., Giepmans, B. N., Palmer, A. E., and Tsien, R. Y. (2004) Improved monomeric red, orange and yellow fluorescent proteins derived from Discosoma sp. red fluorescent protein. *Nat. Biotechnol.* **22,** 1567–1572
43. Phelan, M. C. (2007) Basic techniques in mammalian cell tissue culture. *Curr. Protoc. Cell Biol.* **36,** 1.1.1–1.1.18
44. Marionneau, C., Brunet, S., Flagg, T. P., Pilgram, T. K., Demolombe, S., and Nerbonne, J. M. (2008) Distinct cellular and molecular mechanisms underlie functional remodeling of repolarizing $K^+$ currents with left ventricular hypertrophy. *Circ. Res.* **102,** 1406–1415
45. Niwa, N., Wang, W., Sha, Q., Marionneau, C., and Nerbonne, J. M. (2008) Kv4.3 is not required for the generation of functional Ito,f channels in adult mouse ventricles. *J. Mol. Cell Cardiol.* **44,** 95–104
46. Norris, A. J., and Nerbonne, J. M. (2010) Molecular dissection of I(A) in cortical pyramidal neurons reveals three distinct components encoded by Kv4.2, Kv4.3, and Kv1.4 $\alpha$-subunits. *J. Neurosci.* **30,** 5092–5101
47. Brunet, S., Aimond, F., Li, H., Guo, W., Eldstrom, J., Fedida, D., Yamada, K. A., and Nerbonne, J. M. (2004) Heterogeneous expression of repolarizing, voltage-gated $K^+$ currents in adult mouse ventricles. *J. Physiol.* **559,** 103–120
48. Clark, B. D., Kwon, E., Maffie, J., Jeong, H. Y., Nadal, M., Strop, P., and Rudy, B. (2008) *Front. Mol. Neurosci.* **1,** DOI 10.3389/neuro.3302.3008.2008
49. Shibata, R., Misonou, H., Campomanes, C. R., Anderson, A. E., Schrader, L. A., Doliveira, L. C., Carroll, K. I., Sweatt, J. D., Rhodes, K. J., and Trimmer, J. S. (2003) A fundamental role for KChIPs in determining the molecular properties and trafficking of Kv4.2 potassium channels. *J. Biol. Chem.* **278,** 36445–36454
50. Zhu, X. R., Wulf, A., Schwarz, M., Isbrandt, D., and Pongs, O. (1999) Characterization of human Kv4.2 mediating a rapidly-inactivating transient voltage-sensitive $K^+$ current. *Recept. Channels* **6,** 387–400
51. Maffie, J., Blenkinsop, T., and Rudy, B. (2009) A novel DPP6 isoform (DPP6-E) can account for differences between neuronal and reconstituted A-type $K^+$ channels. *Neurosci. Lett.* **449,** 189–194
52. Burgoyne, R. D., O'Callaghan, D. W., Hasdemir, B., Haynes, L. P., and Tepikin, A. V. (2004) Neuronal $Ca^{2+}$-sensor proteins. Multitalented regulators of neuronal function. *Trends Neurosci.* **27,** 203–209
53. Ren, X., Hayashi, Y., Yoshimura, N., and Takimoto, K. (2005) Transmembrane interaction mediates complex formation between peptidase homologues and Kv4 channels. *Mol. Cell Neurosci.* **29,** 320–332
54. Anderson, D., Mehaffey, W. H., Iftinca, M., Rehak, R., Engbers, J. D., Hameed, S., Zamponi, G. W., and Turner, R. W. (2010) Regulation of neuronal activity by Cav3-Kv4 channel signaling complexes. *Nat. Neurosci.* **13,** 333–337
55. Anderson, D., Rehak, R., Hameed, S., Mehaffey, W. H., Zamponi, G. W., and Turner, R. W. (2010) Regulation of the KV4.2 complex by CaV3.1 calcium channels. *Channels* **4,** 163–167